Pore Pressures in Base Courses

E. S. Barber and G. P. Steffens,
Division of Physical Research, Bureau of Public Roads

Although it is desirable to keep base courses dry, they usually get wet in spite of efforts to prevent entrance of water or provide drainage. However, the stability of granular material depends more on the state of stress in the pore water than on the amount of water present.

A load applied to wet soil (total pressure) is carried between the soil grains (intergranular pressure) or on the water (pore pressure). Since the strength of soil depends upon the intergranular pressure, any pore pressure reduces the strength because the intergranular pressure equals the total pressure minus the pore pressure.

Therefore, measures which prevent the development of pore pressures may maintain the stability of a base course even though the material stays wet. This requires minimizing the amount of fines without making a material too harsh to place with a uniform high density.

Further research is required to develop more refined design criteria for base courses. This should include the thickness, width, and slope of base courses, the permeability, capillarity, strength and stress-strain relations of base course materials, as well as the ambient conditions of moisture and temperature.

• ON SUNNY DAYS during the spring and summer, water was often observed on the surface of an experimental flexible pavement (*1, 2*) built at Hybla Valley, Va. Beginning about 2 years after construction, water appeared during the early afternoon and disappeared in the evening. This water movement is not attributable to fluctuations of the water table in the subgrade because the test sections of pavement were built on a 5-ft clay fill designed to provide uniform subgrade conditions during the period that static and moving load tests were scheduled. A similar phenomenon had been reported in Texas (*3*) and was attributed to pore pressures related to temperature changes in the base course. Related effects of pore pressures are reported for bituminous surfaces (*4*), roofs (*5*), and paint (*6*).

To study this condition quantitatively, concurrent records were made of barometric pressures and temperatures and manometer pressures at various depths below the surface of the test pavement. Also, fluctuations in the height of the water table in the base course were observed in holes dug through the pavement, and measurements of the height were made simultaneously with other readings for correlation purposes. Ample data on the moisture-density of the base course were available for correlation because this study was conducted during the same period that load tests were made to evaluate the thicknesses of the various sections of flexible pavement.

This paper presents the theoretical relation between temperature and pore pressure, its correlation with field measurements, and general observations on the effect of pore pressures on the stability of base courses.

CALCULATIONS

Effects of Temperature Changes on Air-Water Mixtures

At temperatures above freezing, the voids in a base course are filled with air carrying various percentages of water

vapor and water with dissolved air. The volume of the air-water components for any temperature and pressure condition can be calculated from the gas laws of Boyle, Charles, Dalton, and Henry. For example, a condition in a base course is assumed where the volume of voids for a given volume of base is 100 cc; also, that these voids are filled with 88 cc of water saturated with dissolved air and 12 cc of air saturated with water vapor at 32 F and a pressure of one atmosphere (760 mm mercury).

From the properties of water taken from the International Critical Tables (7), shown in Table 1, and molecular weights of 29 and 18 for air and water, respectively, the following calculations for several assumed temperatures and pressures indicate how the data used later in this report were developed for correlation purposes.

Using a specific volume of water 1.00013 (see Table 1 for 32 F), the weight of 88 cc of water is 87.989 g. The vapor pressure at 32 F is 4.58 mm, which leaves a partial pressure on the dry air of 755.42 mm. The weight of dissolved air by Henry's law, using the solubility of air in water (partial pressure per mole fraction) at 32 F of 3.277×10^7, is 0.00327 g. Since a molecular weight of air occupies 22,400 cc at 760 mm, the density of dry air is, by Boyle's law, 0.001287 g/cc.

TABLE 1

PHYSICAL PROPERTIES OF WATER

Temperature		Specific Gravity	Specific Volume	Viscosity (dyne-sec/cm.^{2}) ($\times 10^{-3}$)	Surface Tension (dynes/cm)	Saturated Vapor		Air Solubility, Partial Pressure /Mole Fraction (mm Hg $\times 10^7$)
						Pressure (mm Hg)	Density (mg/cc)	
F	C							
32	0	0.99987	1.00013	17.94	75.64	4.579	0.00485	3.277
33.8	1	0.99993	1.00007	17.32	75.50	4.926	0.00519	3.361
35.6	2	0.99997	1.00003	16.74	75.35	5.294	0.00556	3.450
37.4	3	0.99999	1.00001	16.19	75.21	5.685	0.00595	3.536
39.2	4	1.00000	1.00000	15.68	75.07	6.101	0.00636	3.624
41	5	0.99999	1.00001	15.19	74.92	6.543	0.00680	3.712
42.8	6	0.99997	1.00003	14.73	74.78	7.013	0.00726	3.803
44.6	7	0.99993	1.00007	14.29	74.64	7.513	0.00775	3.894
46.4	8	0.99988	1.00012	13.87	74.50	8.045	0.00827	3.985
48.2	9	0.99981	1.00019	13.48	74.36	8.609	0.00882	4.076
50	10	0.99973	1.00027	13.10	74.22	9.209	0.00941	4.168
51.8	11	0.99963	1.00037	12.74	74.07	9.844	0.01002	4.257
53.6	12	0.99952	1.00048	12.39	73.93	10.518	0.01067	4.347
55.4	13	0.99940	1.00060	12.06	73.78	11.231	0.01135	4.438
57.2	14	0.99927	1.00073	11.75	73.64	11.987	0.01206	4.525
59	15	0.99913	1.00087	11.45	73.49	12.788	0.01283	4.612
60.8	16	0.99897	1.00103	11.16	73.34	13.634	0.01364	4.701
62.6	17	0.99880	1.00120	10.88	73.19	14.530	0.01447	4.789
64.4	18	0.99862	1.00138	10.60	73.05	15.477	0.01536	4.874
66.2	19	0.99843	1.00157	10.34	72.90	16.477	0.01631	4.964
68	20	0.99823	1.00177	10.09	72.75	17.535	0.01730	5.044
69.8	21	0.99802	1.00198	9.84	72.59	18.650	0.01835	5.130
71.6	22	0.99780	1.00221	9.61	72.44	19.827	0.01942	5.216
73.4	23	0.99757	1.00244	9.38	72.28	21.068	0.02058	5.297
75.2	24	0.99733	1.00268	9.16	72.13	22.377	0.02178	5.379
77	25	0.99707	1.00293	8.95	71.97	23.756	0.02304	5.468
86	30	0.99568	1.00434	8.00	71.18	31.824	0.03035	5.858
95	35	0.99406	1.00598	7.21	70.38	42.175	0.03960	6.249
104	40	0.99225	1.00782	6.54	69.56	55.324	0.0511	6.611
113	45	0.99024	1.00985	5.97	68.74	71.88	0.0656	6.916
122	50	0.98807	1.01207	5.49	67.91	92.51	0.0832	7.188
131	55	0.98573	1.01448	5.07	67.05	118.04	0.1046	7.43
140	60	0.98324	1.01705	4.70	66.18	149.38	0.1305	7.64
149	65	0.98059	1.01979	4.37	65.3	187.54	0.1615	7.83
158	70	0.97781	1.02270	4.07	64.4	233.7	0.1984	7.98
167	75	0.97489	1.02576	3.81	63.5	289.1	0.2421	8.09
176	80	0.97183	1.02899	3.57	62.6	355.1	0.2938	8.17
185	85	0.96865	1.03237	3.36	61.7	433.6	0.3541	8.21
194	90	0.96534	1.03590	3.17	60.8	525.8	0.4241	8.22
203	95	0.96192	1.03959	2.99	59.8	633.9	0.505	8.20
212	100	0.95838	1.04343	2.84	58.8	760.0	0.598	8.16

Using this value, the weight of dry air in 12 cc of saturated air is 0.01544 g.

If the temperature is raised to 68 F and the total pressure remains constant at 760 mm, the volume of water becomes 88.145 cc, the vapor pressure becomes 17.54 mm, and the partial pressure of the dry air is reduced to 742.46 mm. With the solubility coefficient decreased to 5.044×10^{7}, the weight of the dissolved air becomes 0.00209 g and releases 0.00118 g to make the total free air 0.01662 g. At 68 F the density of dry air, by Charles' law, is 0.001180 g/cc. The volume of dry air, using this calculated value of density is 14.080 cc. Thus the total volume becomes 102.23 cc which is an expansion of 2.23 percent in the air-water mixture when the temperature is changed from 32 F to 68 F.

Using a coefficient of cubical expansion of stone 18×10^{-6} per degree F, this 36 F temperature change would cause, at the most, an expansion of 0.07 percent which is negligible compared to the 2.23 percent increase of volume in the air-water mixture from 32 F to 68 F.

If the temperature is held constant at 68 F while the pressure is increased 25.4 mm (13.6 in. of water), the dissolved air in water is increased by 0.00007 g, leaving 0.01655 g dry air. The volume of this weight of free dry air is 13.56 cc, and therefore the total volume of water and air becomes 101.71 cc.

Similar calculations for various temperatures and pressures provide data for Figures 1, 2 and 3, which show the relations between temperature, pressure, and volume for an air-water mixture of constant composition. In these calculations, zero gage pressure is taken as 760 mm mercury.

The rates of change of volume with temperature for various air-water compositions are shown in Figure 4, and Figure 5 shows the amount of free air at various temperatures for several air-water compositions. The relation between pressure increase and temperature increase for various compositions at a constant volume with zero initial gage pressure is shown in Figure 6. In Figure 4, the volume increase per degree F increase becomes greater as the relative amount of free air increases. On the other hand, Figure 6 shows that the pressure increase per degree F increase is at a maximum for zero free air and decreases with greater amounts of free air.

Pore Pressures from Cyclical Temperature Changes

If the temperature varies with time and conditions are such that there is no movement of water and escape of air from a base course, the changes in pore pressure will be proportional to the temperature change (Fig. 6) for various air-water mixtures. However, if the pressure changes in the voids and the conditions are such that the downward movement of air or water from a wide thin dense base course is obstructed, either by relatively impervious fine-grained subgrade material or a frozen saturated sand, it will slowly drain laterally with the tendency to move upward through or into the upper part of a less saturated base.

This latter condition simulates a system corresponding to that occurring in a one-dimensional consolidation test with one impervious face, that is impervious boundaries at the bottom and sides of the base course and a reservoir of high permeability at the top (surface), except that the coefficient of consolidation, c_v, is taken as the permeability divided by the compressibility of the air-water mixture in an incompressible base course instead of the permeability divided by the compressibility of the base course with incompressible water. Assume that the base (thickness H) is subjected to a sinusoidal temperature change of unit period with uniformity in temperature changes from top to bottom of the base such that with no drainage the pressure would be $2\pi(t+x)$ (Fig. 7).

Under these conditions, consider an increment of applied pressure, $dp = 2\pi \cos 2\pi(t+x)\,dt$ which is constant to time zero; at time zero, the effect of dp is re-

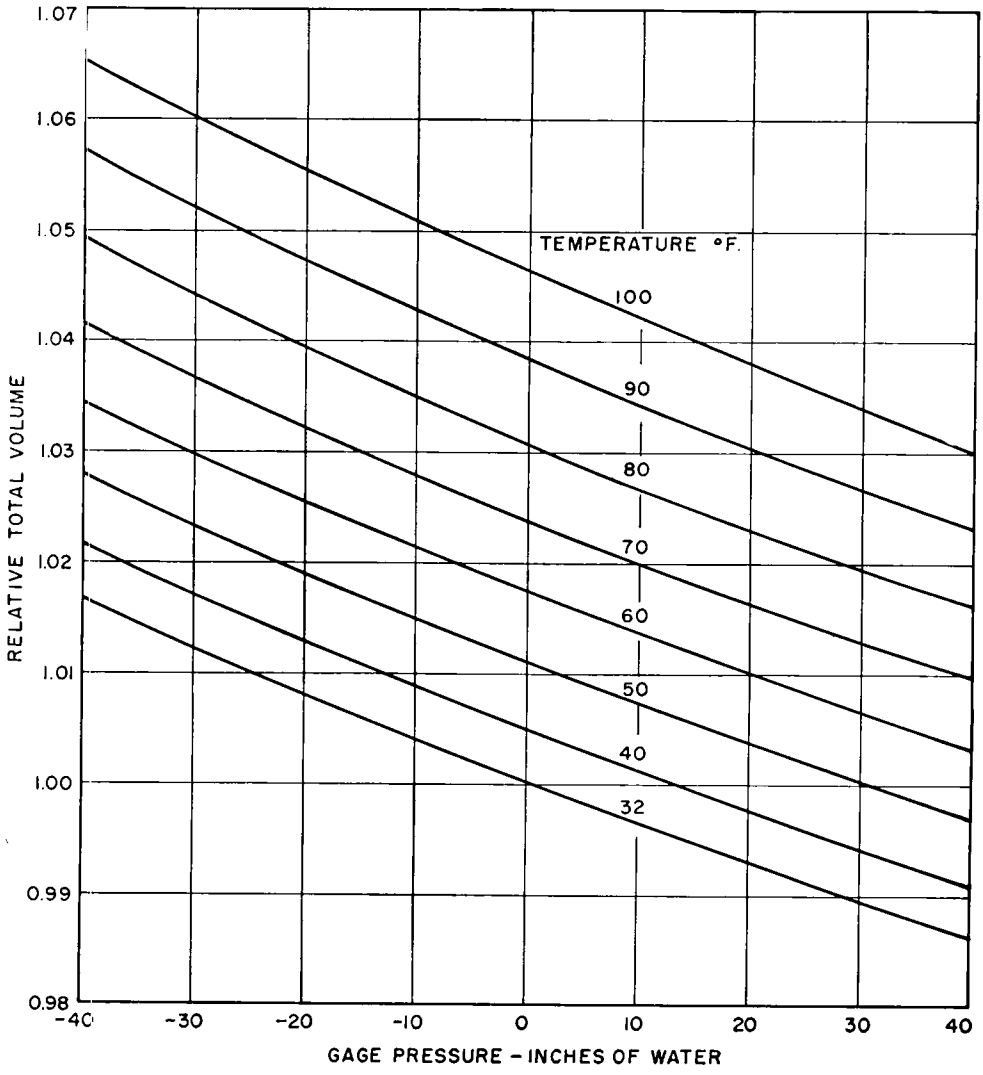

Figure 1. Volume vs pressure for 0.88 volumes of water and 0.12 volumes of air (at 32 F and 0 gage).

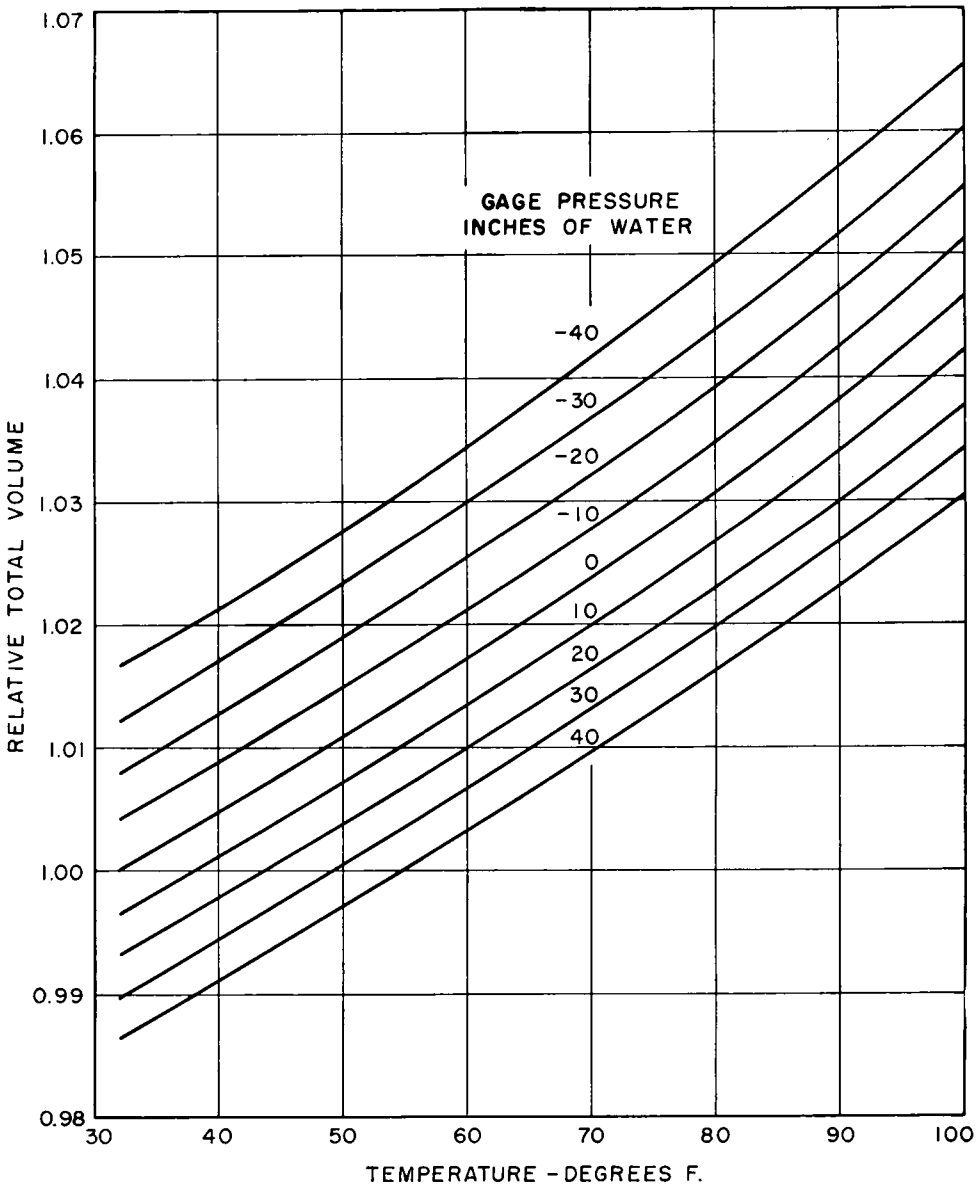

Figure 2. Volume vs temperature for 0.88 volumes of water and 0.12 volumes of air (at 32 F and 0 gage).

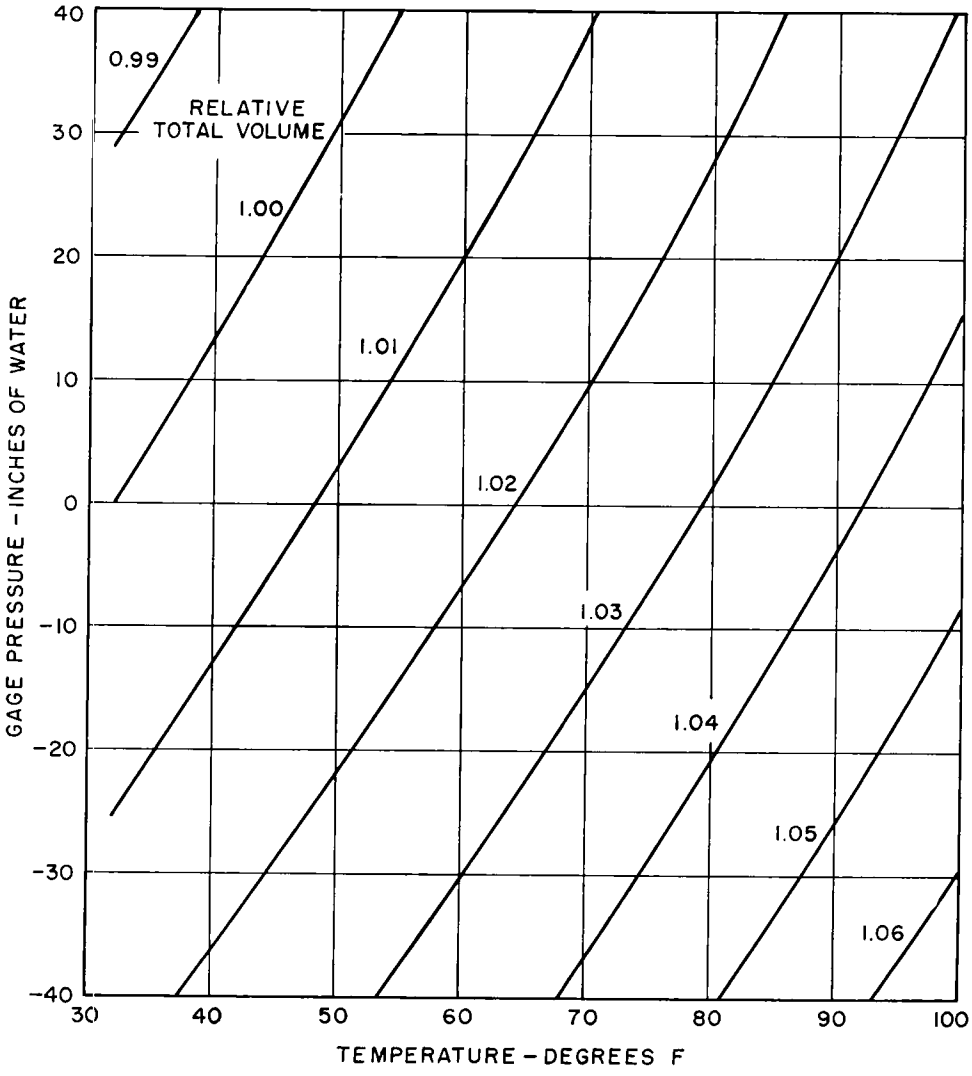

Figure 3. Pressure vs temperature for 0.88 volumes of water and 0.12 volumes of air (at 32 F and 0 gage).

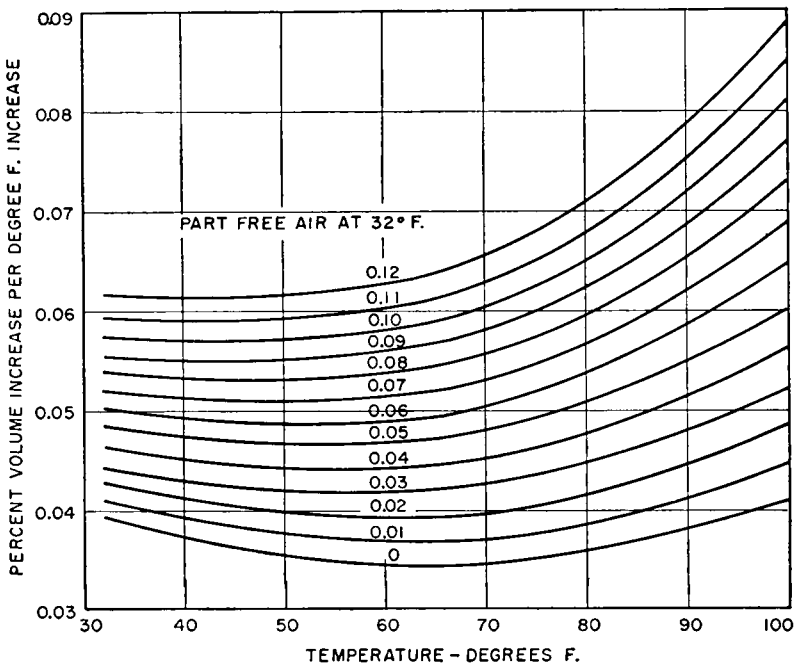

Figure 4. Volume increase with temperature at 0 gage pressure for various air-water mixtures.

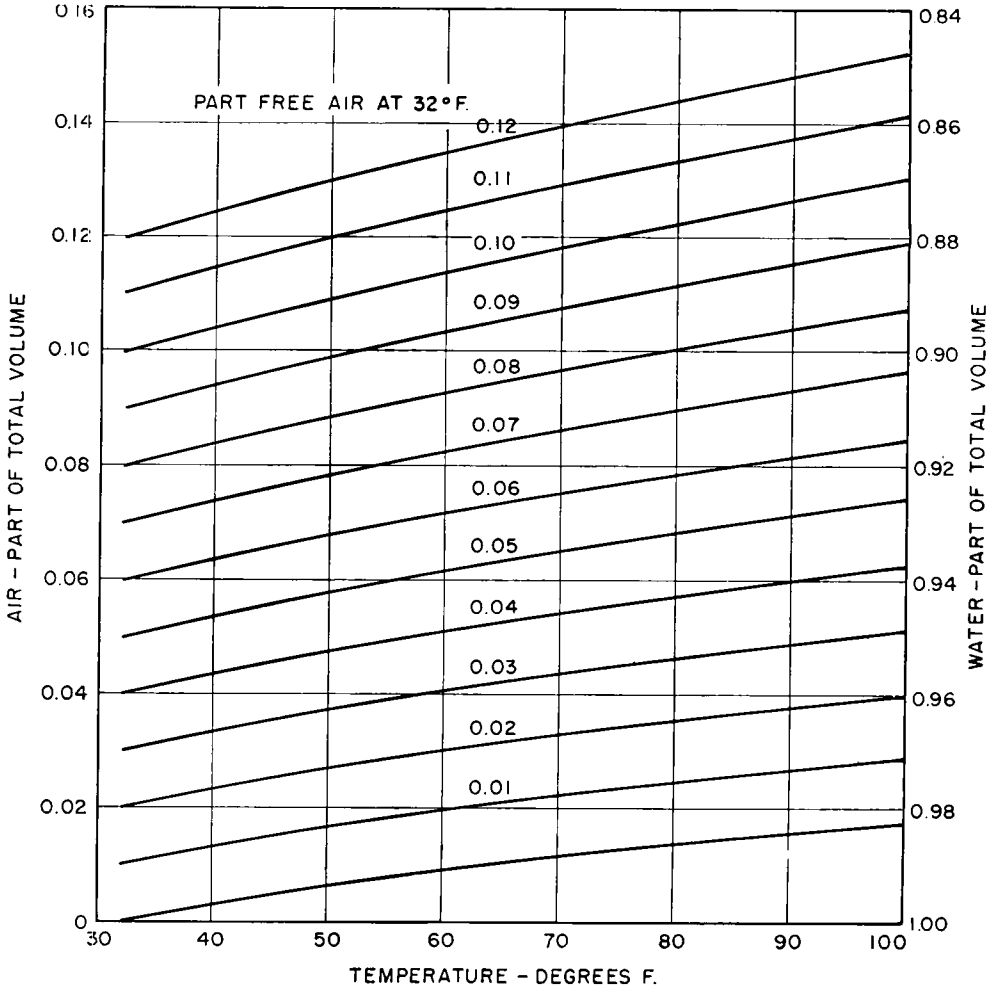

Figure 5. Composition of air-water mixtures (0 gage pressure).

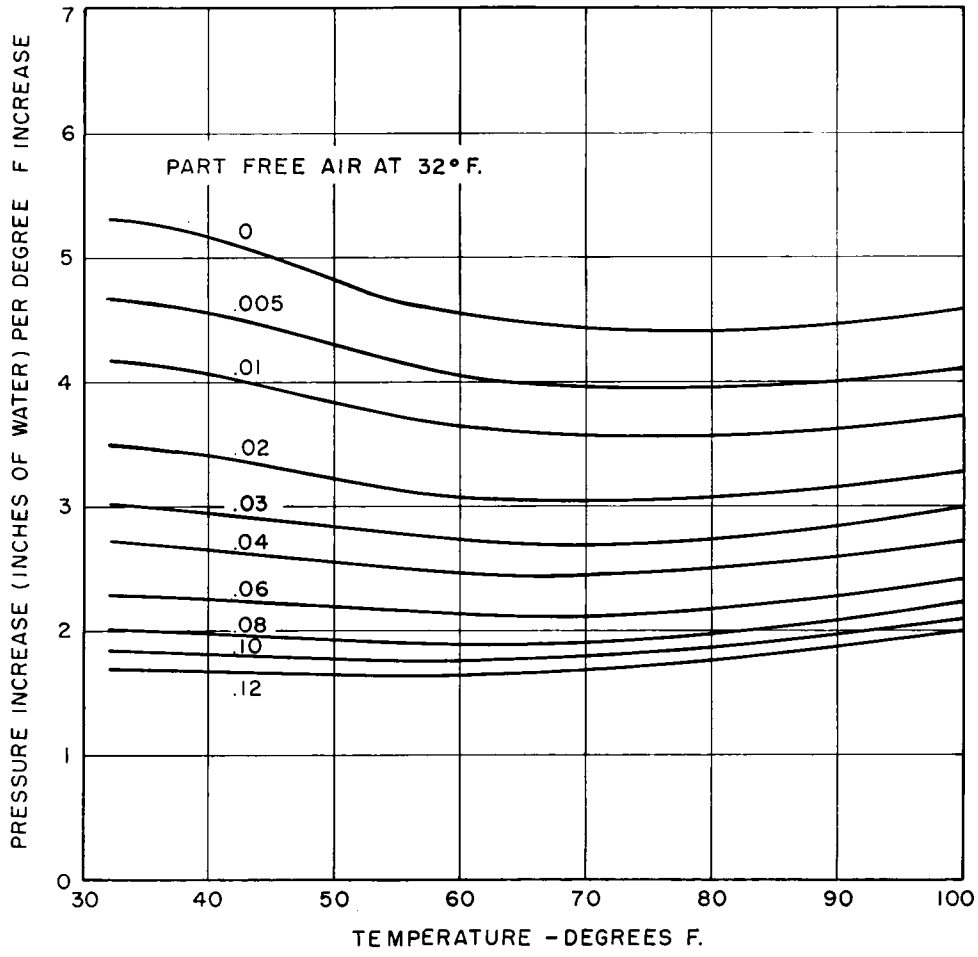

Figure 6. Pressure increase with temperature at constant volume for various air-water mixtures.

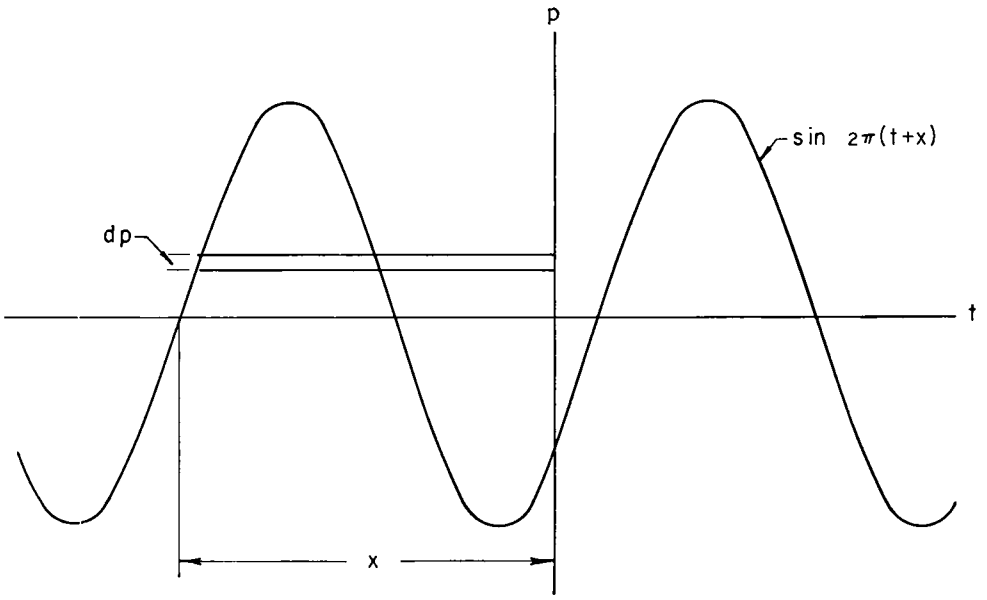

Figure 7. Cyclical pressure applied with no drainage.

duced by the degree of consolidation to dp'. The reduced pressure [1] is

$$dp' = 2\pi \cos 2\pi(t+x) \sum_{n=1,3,5\ldots} \frac{4}{\pi n} e^{M} \sin \frac{n\pi z}{2H}\, dt$$

in which $M = -\dfrac{n^2\pi^2 c_v t'}{4H^2}$, $t'(=-t)$ is the elapsed time from pressure application to time zero, and z is the depth below the upper permeable boundary. Considering the impervious boundary ($z = H$) and expanding $\cos 2\pi(t+x)$ to $(\cos 2\pi t \cos 2\pi x - \sin 2\pi t \sin 2\pi x)$, the total resulting pressure at time zero, assuming the application of pressure to have started at minus infinity, is:

$$p' = \sum_{m=1,-3,5\ldots} \frac{8}{m} \int_{-\infty}^{0} (\cos 2\pi t \cos 2\pi x - \sin 2\pi t \sin \pi 2x)\, e^{N} dt$$

in which

$$N = \frac{m^2\pi^2 c_v t}{4H^2}.$$

[1] From *Public Roads*, March 1937, p. 16, Eq. 46.

By integration $p' =$

$$\sum_{m=1,-3,5\ldots} \frac{8}{m} \frac{\dfrac{m^2\pi^2}{4}\dfrac{c_v}{H^2}\cos 2\pi x + 2\pi \sin 2\pi x}{m^4 \dfrac{\pi^4}{16}\left(\dfrac{c_v}{H^2}\right)^2 + 4\pi^2}$$

or $p' = A \cos 2\pi x + B \sin 2\pi x$

where $A = \displaystyle\sum_{m=1,-3,5\ldots} \frac{\dfrac{m}{2}\left(\dfrac{c_v}{H^2}\right)}{1+\left(\dfrac{c_v}{H^2}\right)^2 \dfrac{\pi^2}{64} m^4}$

and $B = \displaystyle\sum_{m=1,-3,5\ldots} \frac{4/\pi m}{1+\left(\dfrac{c_v}{H^2}\right)^2 \dfrac{\pi^2}{64} m^4}$

A and B have been numerically calculated for various values of c_v/H^2 as shown in Table 2. By combination,

$$p' = \sqrt{A^2+B^2}\, \sin(2\pi x + \text{arc tan } A/B)$$

which is a sine wave with an amplitude of $\sqrt{A^2+B^2}$ and a maximum occurring $\dfrac{\text{arc tan A/B}}{2\pi}$ *before* the maximum for no drainage. The calculated amplitudes ($\sqrt{A^2+B^2}$) and phase displacements

TABLE 2
FACTORS FOR CYCLICAL PRESSURE CHANGE

c_v/H^2	A	B	$\sqrt{A^2+B^2}$	$\frac{\text{arc tan } A/B}{2\pi}$	Abscissa of Maximum
0	0	1.000	1.000	0	0.250
0.1	−0.005	0.994	0.994	−0.001	0.251
0.2	−0.028	1.026	1.026	−0.004	0.254
0.3	−0.007	1.078	1.078	−0.001	0.251
0.5	0.096	1.132	1.136	0.013	0.237
1	0.341	1.074	1.127	0.049	0.201
2	0.569	0.780	0.966	0.100	0.150
5	0.495	0.261	0.559	0.173	0.077
10	0.295	0.077	0.304	0.209	0.041
20	0.154	0.020	0.156	0.229	0.021
50	0.063	0.003	0.063	0.242	0.008
100	0.031	0.001	0.031	0.246	0.004

$\left(\frac{\text{arc tan } A/B}{2\pi}\right)$ of the resultant sinusoidal pressure curves for various values of c_v/H^2 are shown in Table 2.

In Figure 8 the sinusoidal pressure curve for no drainage ($c_v/H^2 = 0$) is shown starting at time zero with a pressure of zero increasing to a maximum relative pressure of 1.00 at 0.25 cycles and then decreasing to zero pressure at 0.50 cycles. This curve is shown because it is used as a base for calculating the relative amplitudes and phase displacements for other values of c_v/H^2. The peaks of the curves for various drainabilities are shown (Fig. 8) by the points on the line denoted as locus of maximum pressures. For comparative purposes a complete half-cycle is also shown for $c_v/H^2 = 1$.

For zero permeability ($c_v/H^2 = 0$)

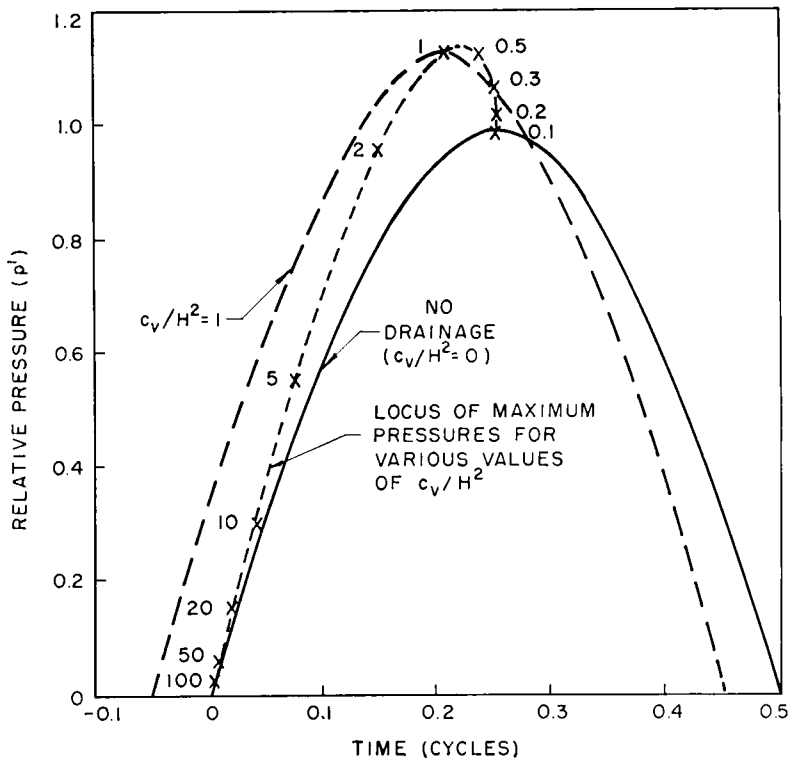

Figure 8. Effect of drainage on cyclical pressure.

there is, of course, no drainage of pore water and for very high permeability (high c_v/H^2) the pressure is lost by the escape of water. It is noted that when c_v/H^2 is less than 2, the maximum pressure is greater with drainage than with no drainage. Also, the maximum pressure precedes the maximum temperature (pressure with no drainage) when c_v/H^2 is greater than 0.3.

Temperature and Pore Pressure Measurements

A flexible pavement, consisting of various thicknesses of gravel base (8 percent passing No. 200 sieve after construction) and a bituminous concrete surface was constructed over a well-compacted fill of relatively impervious clay at Hybla Valley by the Bureau of Public Roads.

A comprehensive testing program of static and moving loads was conducted over a period of about 5 years. Several years after the pavement was built, a series of pressure and water table fluctuation measurements were made in the base course because of the movement of free water from the base course through the bituminous concrete surfacing during the spring and summer.

Temperatures at various depths were measured with thermistors, and water pressures were measured with water manometers. Measurements of the fluctuations in the height of the free water table in the base course were recorded simultaneously with pressure and temperature readings to assemble data from which the graphs shown in Figure 9 were developed (*8*).

A study of the data (Fig. 9) indicates that the temperatures measured at the top and bottom of the base course are cyclic in nature and that the amplitude of the temperature fluctuations decreases with depth below the top of the base course. The temperature at the bottom of the base course lags behind the top of the base because of the insulating effect of the base course.

The pore pressure measured by the manometers and the water level observed in the 4-in. diameter holes dug through the pavement and base course also show a cyclic fluctuation and follow the same general trend observed for the temperatures at the top and bottom of the base course. The height of water in the 4-in. diameter holes is a reflection of the water table but is considerably damped due to the capacity of the holes.

The surface elevation of the pavement also increased slightly with increased temperatures.

The average of 16 measurements on the base course gave a dry density of 143.9 pcf and a moisture content of 5.3 percent. With a measured specific gravity of 2.66 the voids are computed to be 13.3 percent of the total volume. This average moisture content, calculated for 90 F conditions, shows that the voids are comprised of 0.92 parts of water. Using Figure 5, this corresponds to about 0.06 parts of free air at 32 F and from Figure 6, this corresponds to a pressure increase of 2.3 in. water for 1 deg rise in temperature at approximately the 90 F condition. The change in pore pressure for a no-drainage condition in the 12-in. base course can be calculated from the temperature and barometer readings shown in Table 3.

For example, at one o'clock on August 26, the temperature increase from the initial readings (taken at 7 AM, Aug. 25) is 3.7 F (92.2 − 88.5); the corresponding pore pressure increase is 8.5 (3.7×2.3). However, since the barometric pressure during this period changed 0.15 mm (30.02 − 29.87), the pore pressure due to the temperature change of 3.7 F is increased by 2.0 in. (0.15×13.6) giving a total of 10.5 in. which, added to the initial pressure reading of −0.3 in., gives a calculated pore pressure of 10.2 in. The calculated pressures shown in the sixth column of Table 3 were computed in a similar manner and are compared with the observed manometer pressure readings in Figure 10.

Water was observed at the surface of the 3-in. bituminous surface on the 12-in. base course on August 25. However, the maximum manometer reading observed was 13.3 in. during the same period.

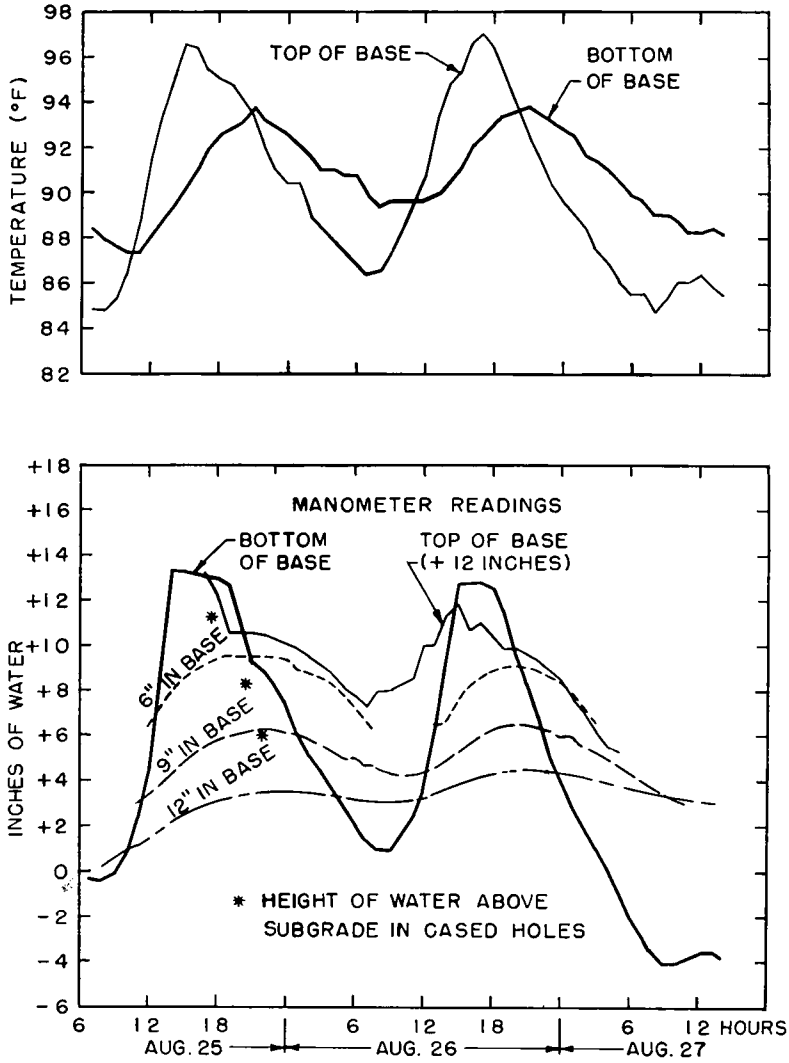

Figure 9. Temperatures and water levels in 12-in. base course for 55-hr period.

Temperature and pressure data shown in Figure 9 indicate that the temperature measured at the top of the base course increases more rapidly than the corresponding temperature measured at the bottom of the base course and is of a greater magnitude. This effect would tend to result in an increase in the pore pressure measured by the manometer at the bottom of the base course.

The lower values in the manometer readings can partially be explained by the fact that some flow of water is required before the manometer registers. Furthermore (as shown in Fig. 8 for example) at $c_v/H^2=1$, the maximum measured pressure develops before the maximum pressure calculated for a no-drainage condition in the base course ($c_v/H^2 = 0$). Although there is a time lag between the manometer readings and the calculated pore pressures for the no-drainage condition (Fig. 10), it is obvious that there is a direct relation be-

TABLE 3

CALCULATION OF PRESSURE AT BOTTOM OF 12-IN. BASE COURSE

Day 1954	Hour EST	Bottom of Base Course		Barometer Reading (in. Hg)	Calculated Pressure [1] (in. H_2O)
		Manometer (in. H_2O)	Temperature (F)		
Aug. 25	7	−0.3	88.5	30.02	−0.3 [2]
	9	−0.1	87.7	30.02	−2.1
	11	2.3	87.4	30.00	−2.5
	13	8.9	88.8	29.97	1.1
	15	13.3	90.2	29.93	4.8
	17	13.1	92.0	29.89	9.5
	19	12.7	92.9	29.89	11.6
	21	9.3	93.8	29.91	13.4
	23	8.2	92.9	29.89	11.6
Aug. 26	1	6.1	92.2	29.87	10.2
	3	4.4	91.1	29.86	7.9
	5	2.9	90.8	29.87	7.0
	7	1.4	89.9	29.87	4.9
	9	0.9	89.7	29.92	3.9
	11	2.4	89.4	29.92	3.2
	13	6.2	89.9	29.92	4.3
	15	12.7	91.1	29.90	7.3
	17	12.8	92.6	29.91	10.6
	19	11.5	93.5	29.92	12.6
	21	8.3	93.8	29.96	12.7
	23	5.2	93.2	29.99	10.9
Aug. 27	1	2.9	92.6	30.03	9.0
	3	1.1	91.4	30.03	6.3
	5	−0.8	90.5	30.04	4.0
	7	−2.8	89.7	30.07	1.8
	9	−4.0	89.1	30.10	0
	11	−3.8	88.3	30.12	−2.2
	13	−3.4	88.5	30.13	−1.8

[1] On the basis of temperature and barometric pressure, with constant air-water composition.
[2] Assumed equal to manometer reading.

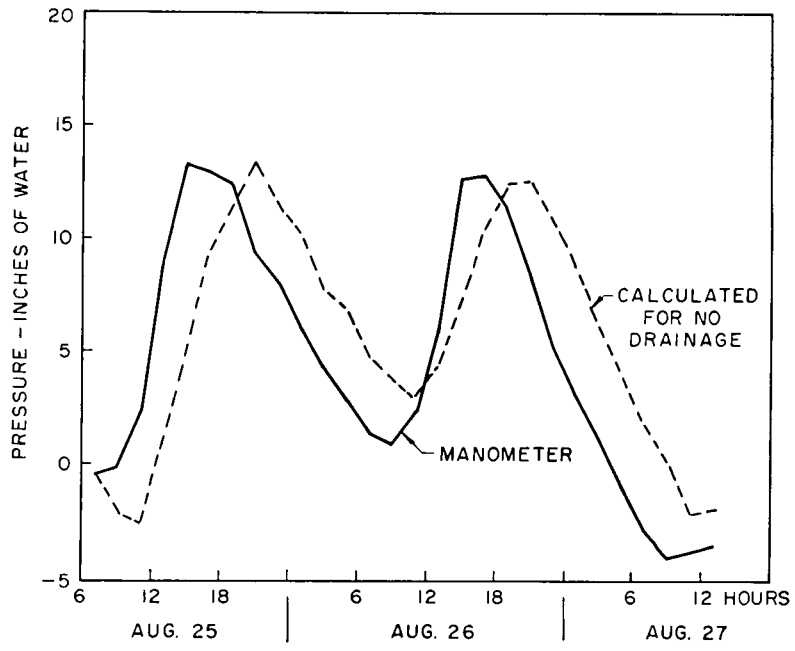

Figure 10. Measured and calculated pore pressures.

tween temperature and pore pressure occurring in the base course.

Smaller pressure and temperature changes were measured in an 18-in. base course and much higher pressure changes would be expected in a 6-in. base course because of the greater temperature changes.

A series of observations of pressure and temperature were made over a period of 4 weeks excluding weekends and are shown in Table 4 for comparative purposes. To evaluate these data, it was necessary to make several assumptions which are as follows:

1. Constant climatic conditions were assumed prior to August 30, and linear interpolation was used to estimate conditions over weekends.
2. The calculations of pressure were based on a constant air-water composition.
3. Zero time lag was assumed in making the comparison of maximum measured pressures with maximum calculated pressures.
4. A mean pressure of one atmosphere, 760 mm mercury, was assumed as a base for calculating daily cyclical changes in pore pressure.
5. To compensate for the changing daily mean temperature and barometric pressure, a 4-day lag with a parabolic decrease with time was assumed to calculate the daily effective mean temperature and barometric pressure.

This adjustment is based on the fact that after the rains from September 17-21, the average manometer reading was above zero for about 4 days until the excess water which entered through the surface seeped out laterally. With the assumed 4-day lag with a parabolic decrease with time, the effective temperature and barometric differential for previous days is the sum of 0.55, 0.35, 0.20 and 0.10 times the respective change in the average of the barometer and temperature changes for the previous 1, 2, 3 and 4 days.

Hourly readings were taken from 8 AM to 11 PM on each week day for the 4-week period. The daily minimum and maximum temperature at the bottom of the 12-in. base were obtained. Because of the limited amount of data, only about two-thirds of each daily cycle, it was necessary to use the half-range of the daily temperature cycle $\left(\frac{\max - \min}{2}\right)$ and similarly the half-range of daily barometric pressure cycle to develop data for correlation purposes.

The calculated half-range in pressure is as before the sum of the barometer and temperature effect. It approximates the half-range in manometer readings when they were determined (the manometer often failed to read the negative minimum pressure).

The temperature and barometer trends in terms of inches of water pressure (Table 4) are reflected in the calculated effective temperature and barometer (Fig. 11). Adding the trend effects to the half-range gives the calculated maximum pressures which are compared with the maximum manometer readings in Figure 11. A good correlation is seen except for the period after rains. The calculated values are for constant water content so that any increase in water content due to infiltration of rainwater will temporarily make the measured pressures higher than those calculated. Thus, when the water depth in the 4-in. diameter hole rises (despite a fall in temperature) as on August 31 and September 20-22 due to the previous rain, the manometer readings are above the calculated pressures. This is especially noticeable for the last week where 3 or 4 days are required for the effects of infiltration to dissipate.

If the base course did not maintain almost a constant degree of saturation from top to bottom by capillarity, the volume change required to raise the water table would relieve much of the pressure. Figure 12 shows the moisture content after one day of drainage of a column of the passing No. 10 sieve fraction of the base course material compacted to the equivalent density that the fraction passing the No. 10 sieve had in the compacted base course.

TABLE 4

PRESSURES AND TEMPERATURES FOR 4 WEEKS AT BOTTOM OF 12-IN. BASE COURSE

Date 1954	Barometer		Temperature		Calculated ½ Range (in. H_2O)	Manometer		Temp. Trend (in. H_2O)	Barometer Trend (in. H_2O)	Calculated Maximum Pressures (in. H_2O)
	Mean 8-18 hr (in. Hg)	Diff. at 18 hr (in. H_2O)	Mean, Max & Min (F)	½ range × 2.3 (in. H_2O)		½ range (in. H_2O)	Max (in. H_2O)			
Aug. 30	29.86	1.1	88.6	5.1	6.2	—[1]	7.4	0	0	6.2
31	29.79	—1.0	86.7	4.3	3.3	5.2	7.5	—2.5	0.5	1.3
Sept. 1	30.07	0.4	85.6	8.6	9.0	—	7.6	—2.8	—1.8	4.4
2	30.08	1.0	86.7	9.4	10.4	—	9.5	—0.4	—1.2	8.8
3	29.94	0.5	88.0	8.5	9.0	—	12.1	1.6	0.3	10.9
7	29.98	0.7	93.5	7.5	8.2	8.6	13.5	3.8	—0.2	11.8
8	30.01	0.1	92.3	4.1	4.2	5.7	6.9	0.6	—0.3	4.5
9	30.06	0.4	90.3	2.6	3.0	4.0	1.8	—2.6	—0.6	—0.2
10	29.90	1.1	88.4	2.3	3.4	—	0.6	—4.2	0.9	0.1
13	30.24	1.2	83.3	8.4	9.6	—	4.1	—4.8	—1.5	3.3
14	30.14	0.5	84.1	8.3	8.8	—	4.3	—1.5	—0.3	7.0
15	30.17	0.5	84.2	2.5	3.0	—	0.7	—0.4	—0.2	2.4
16	30.08	0.8	84.5	8.1	8.9	6.3	11.1	0.5	0.6	10.0
17	30.06	0.7	86.0	7.1	7.8	8.3	11.9	2.4	0.6	10.8
20	29.73	—0.1	81.7	1.6	1.5	5.2	11.8	—3.3	1.7	—0.1
21	29.63	1.4	79.1	2.8	4.2	5.0	9.6	—5.4	1.7	0.5
22	29.93	—0.3	77.8	7.4	7.1	7.7	12.5	—4.7	—1.3	1.1
23	30.19	0.3	77.9	7.1	7.4	7.3	8.3	—2.4	—2.9	2.1
24	30.26	1.1	77.7	9.8	10.9	—	6.5	—1.4	—2.4	7.1

[1] Dash indicates manometer failed to read minimum pressure.

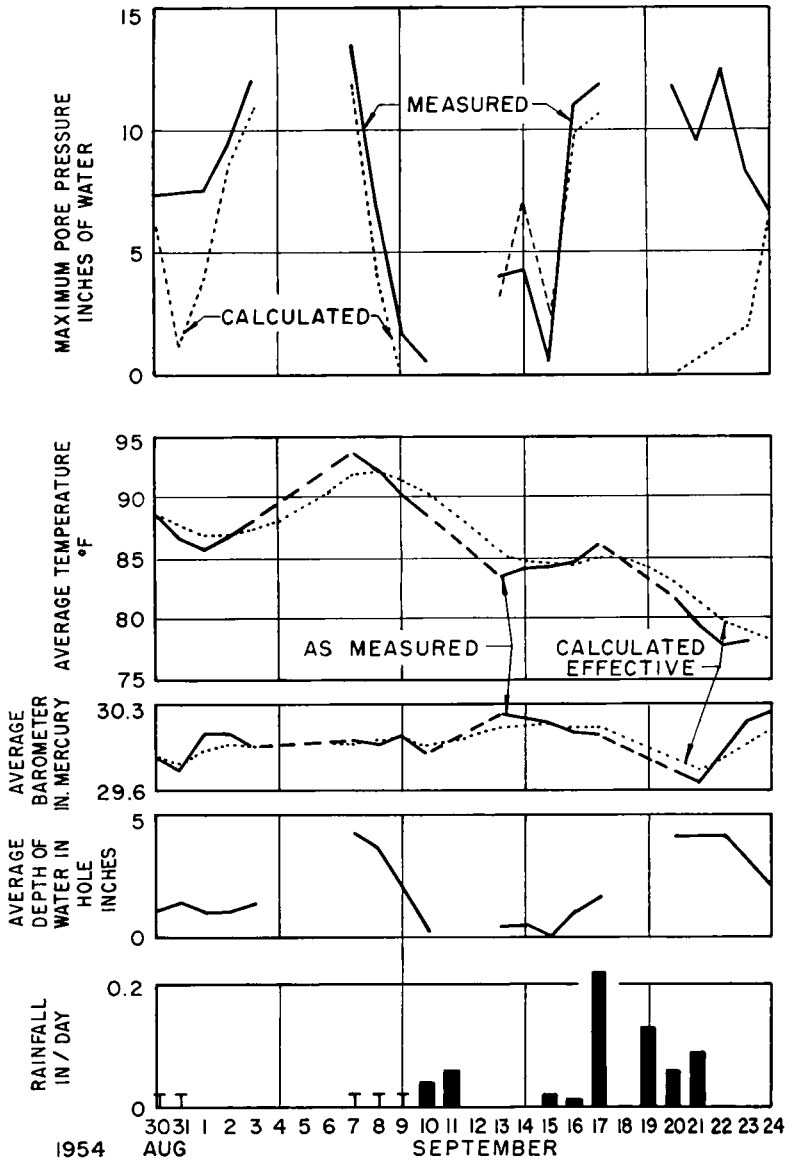

Figure 11. Correlation of calculated pore pressure with measurements.

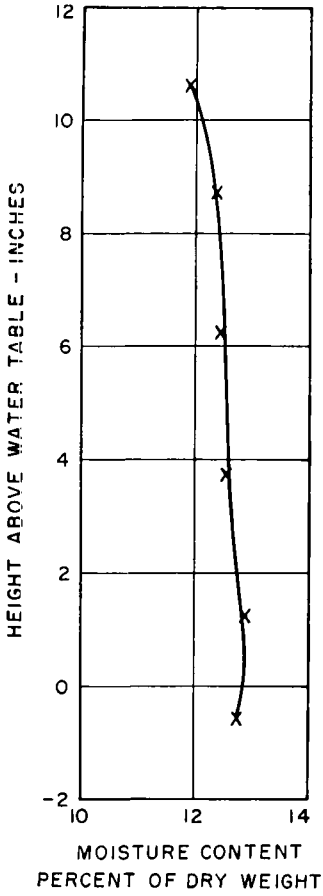

Figure 12. Capillary water retention 24 hr after compaction.

It is apparent from the data (Fig. 12) that the percent of capillary water retained in the minus No. 10 sieve material in the base course is quite uniform (12.8 to 12.0 percent) for the 11-in. height above the free water table measured for the 1-day drainage condition.

Effect of Pore Pressure on Theoretical Bearing Capacity of Base Courses

The effect of pore pressure on the theoretical static bearing capacity (q) of a base course may be calculated for various conditions from the formula and factors shown in Figure 13 (*9*). A 9,000-lb wheel load on dual tires is assumed to produce a circular loaded area under the pavement surface with a radius a' of 5 in. and a pressure p' of 57 psi. Assumed values for the components of the pavement are surface thickness $z = 3$ in., density of the base w' and surface $w = 140$ pcf (0.081 lb per cu in.), and a coefficient of friction $f = 1.0$ for a well-compacted base course.

Before applying the surface z, a noncohesive base course material would have a bearing capacity of $q = 0+0+0.081\times5\times192 = 78$ psi. This provides very little margin of strength and makes such a material difficult to keep in place during construction. A damp stone or gravel base graded down to fine sand could develop a cohesion of 1 psi. (2.3 ft water) due to the surface tension of water. This would increase the bearing capacity to $q = 1\times224+78 = 302$ psi, which greatly increases its resistance to construction displacement. More cohesion could be obtained with the addition of a small amount of clay, but a slight excess would greatly reduce the friction and thereby decrease the bearing capacity when wet.

After surfacing, the moisture in the base course is apt to increase and thereby reduce the cohesion; with the water table at the bottom of a 12-in. base, the cohesion caused by surface tension would average 0.22 psi (6 in. water). The bearing capacity would be $q = 0.22\times224+0.081\times3\times172+78=169$ psi, which is adequate to carry the imposed 9,000-lb wheel load. If a rise in temperature or leaking through the surface raised the water table to the top of the base, the cohesion would be lost, the effective density of the base w' would be reduced by the density of water and the bearing capacity would be reduced to $q = 0+42+(0.081-0.036)\times5\times192 = 85$ psi, which leaves only a small margin of bearing capacity. A temperature increase or other condition which raises the pore pressure to give an effective water table at the top of the pavement surface would further reduce the bearing capacity to $q = 0+(0.081-0.036)\times2\times172+(0.081-0.036)\times5\times192 = 66$ psi, which leaves very little margin of safety. Now assume

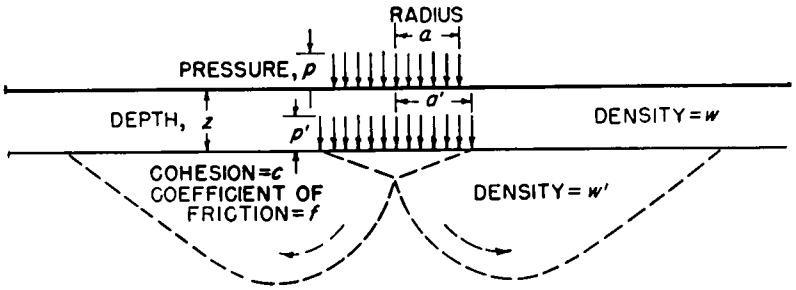

f	Fc	Fz	Fa
0	7.4	0.0	0.0
0.1	9	0.8	0.1
0.2	14	2.1	0.4
0.3	19	4.3	1.2
0.4	27	8	3.0
0.5	36	14	6.6
0.6	53	24	13
0.7	75	40	26
0.8	106	67	51
0.9	156	108	102
1.0	224	172	192

Figure 13. Bearing capacity under circular loaded area.

that a temperature increase or an artesian condition raises the pore pressure to give an effective water table 6.7 in. above the top of the base. This reduces the surcharge effect of pavement to zero or, stated another way, the pavement is floating on a thin film of water between the base course and pavement. The bearing capacity of the base is thereby reduced to $q = 0+0+(0.081-0.036)\times 5\times 192 = 43$ psi, which indicates inadequate bearing capacity.

These calculations for static bearing capacity of a 12-in. granular noncohesive base course (Fig. 14) show reduction of bearing capacity from 169 psi to 66 psi when the effective water table rises from the bottom of the base course to the top of a 3-in. pavement surface. This change in effective water table (pore pressure) of 15 in. could be caused by an increase of the base course temperature of 6.5 F, as shown in previous calculations.

The bearing capacities previously calculated may be compared with that of an open-graded base which stays sufficiently drained so that no cohesion or pore pressure is developed. This type of base (for $f = 1$ and $c = 0$) would have a constant bearing capacity of $q=0(224)+(0.081)(3)(172)+(0.081)(5)(192) = 120$ psi.

Laboratory Tests

The effect of pore pressure on the strength of granular materials can be demonstrated in the laboratory. For instance, CBR tests were run on compacted graded sand with respectively 100, 62, 39, 26 and 5 percent passing the 4, 10, 20, 40 and 200 sieves. The results are as follows:

Water Condition	Surcharge (lb)	Corrected CBR (0.1 in. penetration)
Drained	10	63
Submerged	10	36
Submerged	5	18
Submerged	0	4

Figure 15 shows the decrease in penetration resistance of wet compacted sand when rapidly heated. Less effect is observed in cohesive soils; thus, a clay soil at 120 F had two-thirds the penetration resistance it had at 40 F, which is less than the difference in the viscosity of water (*10*).

At about 85 percent saturation the air permeability increases rapidly with less saturation (Fig. 16).

With increasing moisture content, the optimum moisture for dynamic compaction is reached when the escape of air and water is greatly restricted during the application of load. Therefore, the locus of optimum moistures for most soils and soil-aggregate mixtures (Fig. 17) is at approximately 85 percent of saturation. On the other hand, an optimum moisture is not obtained for materials with very high permeability or for compaction by long-time loading.

At a density of 94 pcf, the subgrade under the WASHO test pavement (*11*) reached a critical condition when the moisture content rose to 23 percent. With a measured specific gravity of 2.55, this is a relative saturation of 85 percent.

Samples of this soil were tested in the soils laboratory of the Bureau of Public Roads. Figure 18 shows the relation between moisture and density for the WASHO subgrade soil and the penetra-

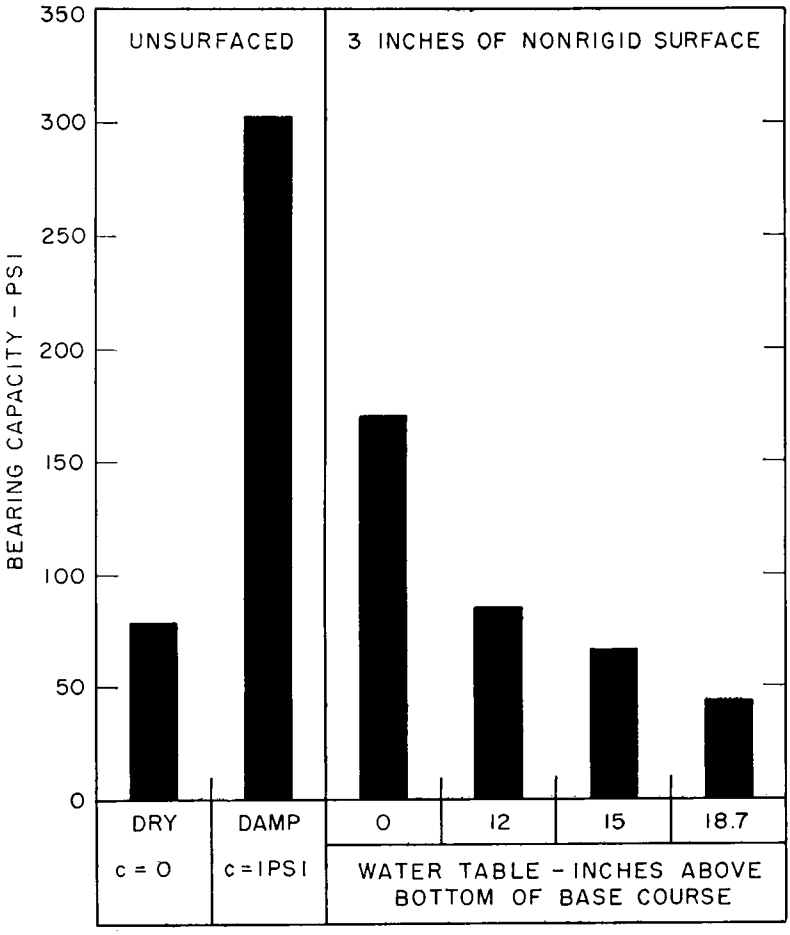

Figure 14. Effect of pore pressure on calculated bearing capacity of a 12-in. base course, $w = w' = 140$ pcf; $f = 1.0$; $a' = 5$ in.

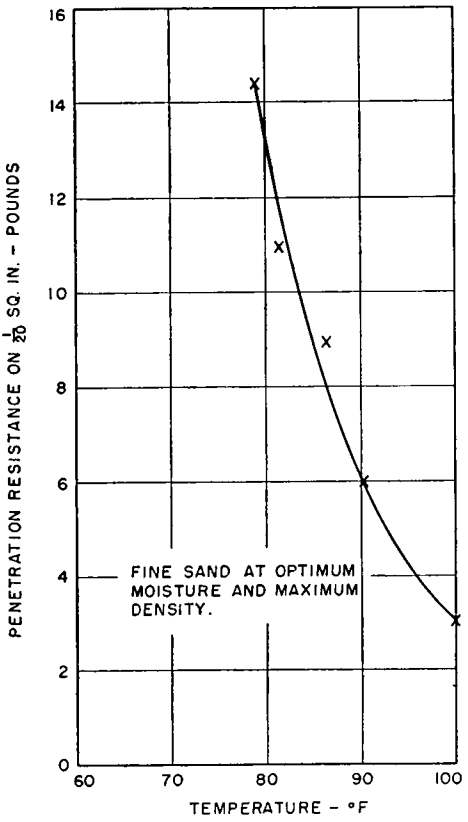

Figure 15. Temperature vs penetration resistance.

tion (0.001 in. of a 2-in. diameter piston loaded with 83 lb and with 5,000-load applications) obtained for various percentages of saturation. A study of these data indicates that samples compacted to less than 85 percent saturation had lower values of penetration than those compacted to more than 85 percent saturation at equivalent moisture contents. Since penetration is a measure of strength, it is apparent that the bearing capacity of this soil is critical at or near 85 percent of saturation for dynamically compacted soils. However, soils statically compacted at the same moisture and density (Fig. 18) have much less penetration and, therefore, have greater bearing capacity. The difference in these two methods of compaction is largely due to shearing during the dynamic compaction of this soil.

In addition to the adverse pore pressure developed with the increased percentage of saturation during loading, there are other related factors which must be considered; namely, (a) the effect of increased percentages of granular material, (b) the increased coefficient of friction resulting from increase in angularity of the granular components of the soil, (c) the effect of density, and (d) the effect of varying the amounts of soil fines (passing No. 200 sieve) in granular materials.

Triaxial strength test data reported for pervious granular materials (*12*) show that the total strength of these materials increases up to 20 percent when the percentage of coarse aggregate above the No. 4 sieve is increased from 0 to 50 percent. Also, when the angularity of the coarse material was changed from rounded to crushed particles there was an additional 10 percent increase in the coefficient of friction. However, the largest variable affecting the strength obtained was the density at which the specimens were tested. The average coefficients of friction obtained by the triaxial compression test for materials of various gradations were 0.76, 0.85, and 0.98 for relative densities of 0.50, 0.70, and 0.90, respectively.

Another investigator (*13*) reported similar advantage of densification of well-graded materials containing 10 percent passing the No. 200 sieve. With 6 percent water and lateral pressures up to 30 psi, the triaxial tests indicated relative strengths of 0.58, 0.85, and 1.00 for dry densities of 126, 136, and 141 pcf, respectively.

The following data taken from an unpublished portion of a report (*14*) show the effect of decreasing the percentage of material passing the No. 200 sieve on compressive strength and stress-strain modulus as measured by the triaxial compressive strength test:

Passing No. 200 Sieve (percent)	Compressive Strength (lateral pressure = 20 psi) (psi)	Stress-Strain Modulus (kips/sq in.)
15	190	5
8	210	8
0	210	11

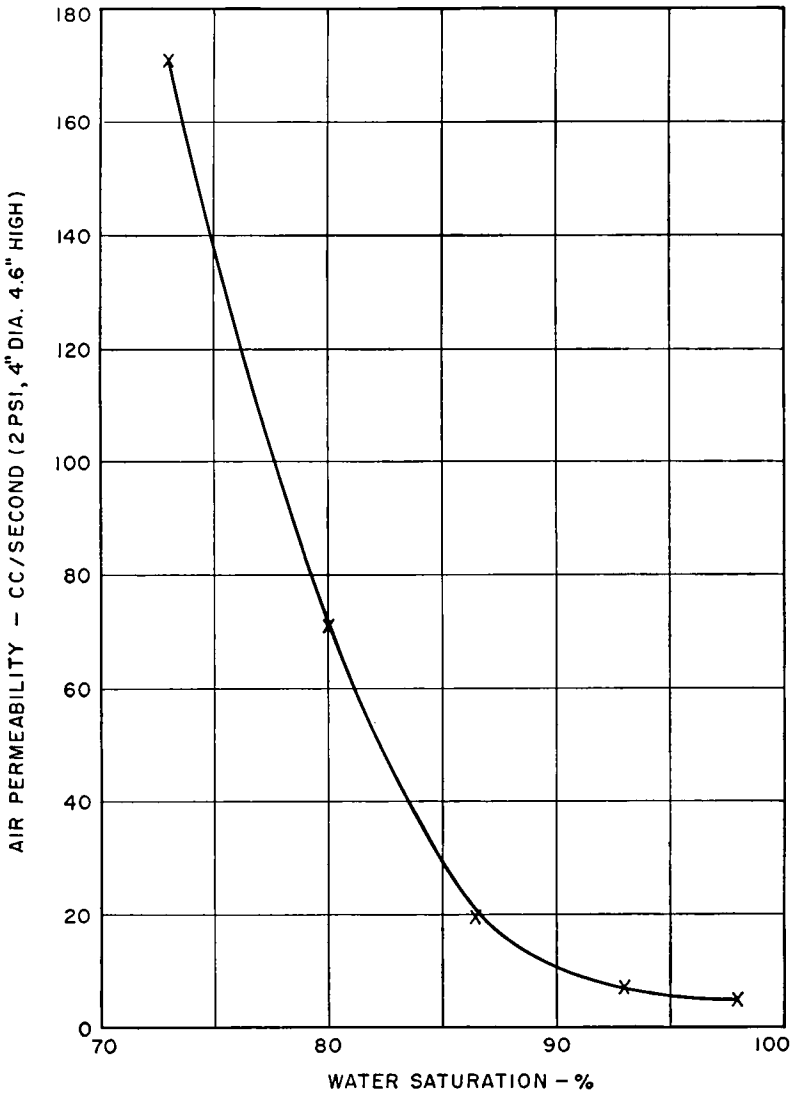

Figure 16. Air permeability vs saturation.

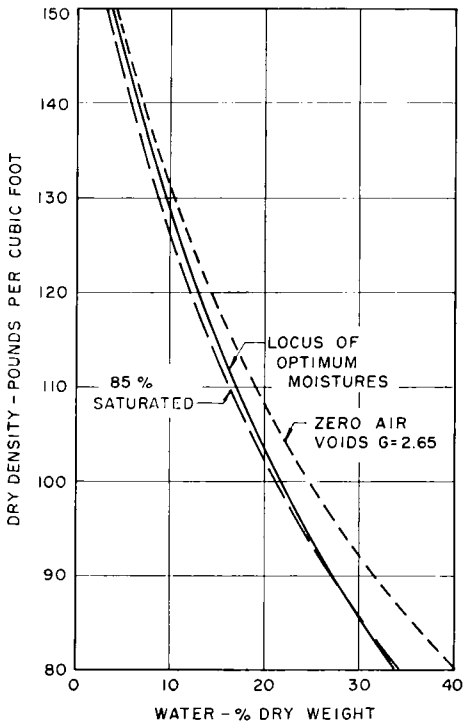

Figure 17. Optimum moisture vs saturation.

A study of the above data indicates that there is a considerable increase in the stress-strain modulus with a decrease in the percentage of soil passing the No. 200 sieve.

A third investigator (*15*) reported that a maximum density of a soil-gravel mixture was obtained with 10 percent passing the No. 200 sieve and a maximum CBR when 7 percent was used.

Field Conditions

Critical pore pressures which affect the bearing capacity of a subgrade or base course can be controlled by changing the gradation and drainage so that the material when compacted has void spaces which are less than 80 percent saturated.

During construction developed pore pressures may cause shearing which reduces the strength of soils in spite of the precautions taken during normal compaction. This effect may be minimized by (a) compacting the soil at moisture contents slightly below standard AASHO optimum for low volume change soils, and (b) using larger roller contact areas to lower unit pressures. For earth dams, compaction 2 percent less than optimum is specified to minimize critical pore pressures in the structure. However, too low an initial moisture content in clay soils will usually cause swelling when the water content increases.

A well-drained condition requires a means of egress of water greater than the potential infiltration from the edges and through the surface. Excess water in a base may be removed downward by flow into a permeable subgrade with a deep water table or lateral flow through a thick permeable base with sufficient outlets to reduce the required distance of lateral flow. Dense-graded bases of usual dimensions generally have insufficient permeability for rapid lateral drainage if saturated.

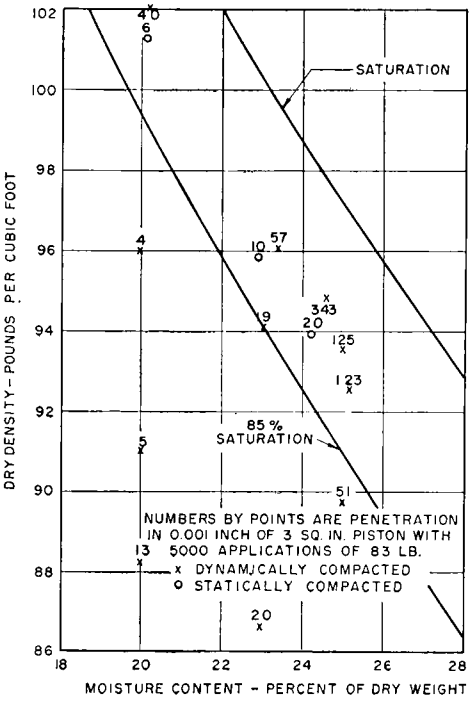

Figure 18. Penetration vs moisture and density.

In nonfrost areas, finer materials have sometimes stood up even with poor drainage. This may be attributable to the tendency for a dense granular material to expand during shearing to overcome the interlocking obtained with compaction beyond the critical density. Thus, a 10 F rise in temperature will cause a pressure of 23 in. water (assuming 6 percent air at 32 F) but if the material expands 0.6 percent of its volume, the pressure is relieved.

This volume change is within the range of expansion of graded granular material compacted to 100 percent of standard compaction. Under dynamic loads, the effect of a standing water table may possibly be counteracted by this same expansion, if loads are not repeated at the same place since high density with limited permeability causes a temporary vacuum to be created by shear expansion.

In regions where deep frost penetration occurs, thawing from the surface will usually prevent downward drainage of the base course for a period of time. Freezing and thawing of a very wet base course may adversely affect its stability unless it has sufficient permeability when it thaws to allow water to escape from under a wheel load without lateral flow of the granular base. This requirement is demonstrated by materials which do not shove in the standard impact compaction test at moisture contents greater than the optimum moisture content (*16*). This criterion generally limits the amount of fines to a maximum of 10 percent passing the No. 200 sieve, and this limit is used in several states. In North Carolina, extra-thick surfaces are required for bases with more than 10 percent passing the No. 200 sieve (*17*). Degradation during and after construction must be considered.

If open-graded base courses are used as insulation against frost, care must be taken to prevent ventilation through the base which can nullify the insulating effect. Such ventilation is the apparent reason for increased frost penetration into the subgrade with increased pavement thickness of the WASHO Road Test (*11*). The density of 132 pcf with an average moisture content of 5 percent corresponds to a degree of saturation of 50 percent which indicates a high air permeability.

REFERENCES

1. BENKELMAN, A. C., AND OLMSTEAD, F. R., "A Cooperative Study of Structural Design of Nonrigid Pavements." *Public Roads,* Dec. 1947.
2. LANCASTER, R. J., AND DRISCOLL, J. E., "A Cooperative Study of Structural Design of Nonrigid Pavements." *Public Roads,* August 1949.
3. SIMONS, C. E., "Research to Form Basis of Future Road Construction." *Texas Parade,* June 1938, p. 3.
4. "Blistering of Asphalt Surfaces." *Road Abstracts,* page 93, September 1938.
5. LUND, C. E., AND GRANUM, R. M., "Principles Affecting Insulated Built-up Roofs." University of Minnesota Bulletin 34 (1952).
6. FISCHER, W. VON, "Paint and Varnish Technology." Reinhold p. 370, (1948).
7. "International Critical Tables, Vol. III." Specific Volume of Water, p. 25; Vapor Pressure, p. 212; Solubility of Air, p. 257.
8. BENKELMAN, A. C., AND WILLIAMS, STUART, "A Cooperative Study of Structural Design of Nonrigid Pavements—Review of Test Procedures and Presentation of Rigid Plate Bearing Test Data." (Third progress report) Appendix B (unpublished).
9. BARBER, E. S., "Triaxial Compression Test Results Applied to Flexible Pavement Design." *Public Roads,* September 1947.
10. HOGENTOGLER, C. A., AND WILLIS, E. A., "Stabilized Soil Roads." *Public Roads,* May 1936.

11. "The WASHO Road Test, Part 2." HRB Special Report 22, 1955.
12. HOLTZ, W. G., AND GIBBS, H. J., "Triaxial Shear Tests on Pervious Gravelly Soils." *Proc.* ASCE, Paper 867 (1956).
13. ALDOUS, W. M., HERNER, R. C., AND PRICE, M. H., "Triaxial Test Data on Structural Properties of Granular Base Materials." CAA Technical Development Report No. 144 (1951).
14. YODER, E. J., AND LOWRIE, C. R., "Triaxial Testing Applied to Design of Flexible Pavement." *Proc. HRB*, Vol. 31, p. 487 (partly unpublished) (1952).
15. YODER, E. J., AND WOODS, K. B., "Compaction and Strength Characteristics of Soil-Aggregate Mixtures." *Proc. HRB*, Vol. 26, p. 511 (1946).
16. MCDONALD, C. H., "Investigation of a Simple Method of Identifying Base Course Material Subject to Frost Damage." *Proc. HRB*, Vol. 29, p. 392 (1949).
17. HICKS, L. D., "Design and Construction of Base Courses." HRB Bulletin 129 (1956).